# 3D-Scattering Center Detection of Automotive Targets Using 77 GHz UWB Radar Sensors

Markus Andres, Peter Feil, Wolfgang Menzel
Institute of Microwave Techniques University of Ulm
89081 Ulm, Germany
markus.andres@uni-ulm.de, peter.feil@alumni.uni-ulm.de, wolfgang.menzel@uni-ulm.de

***Abstract*— 3D scattering center analysis enables to derive radar system specifications for future automotive applications. Synthetic aperture radar (SAR) and SAR in combination with digital beam forming (DBF) will be presented to extract the location of scattering centers at 77 GHz. Furthermore, a mechanical scanning antenna with high directivity is used to compare the reflections of different automotive targets for different elevation and aspect angles.**

***Keywords - automotive radar; scattering center; digital beam-forming; SAR***

## I. INTRODUCTION

Presently, the requirements for advanced automotive safety and driver assistance systems are increasing to avoid or mitigate accidents at an early stage. Radar sensors are commonly used because of their robust detection of obstacles even under adverse weather conditions. Due to diverse highway and urban scenarios, radar sensors have to cope with different target types and scenarios. To realize automatic brake assistances or adaptive cruise control system, they have to observe targets in front and determine their exact location.

Automotive targets have several distributed scattering centers on the outer shell. The reflection center with the highest reflectivity will mainly end up as tracked object after signal processing. The knowledge of the exact location of the scattering centers improves to determine the distance of the target and enables to estimate, at least at smaller distances, the target dimension and orientation. However, several nearby scattering centers are affecting the backscattered radar signal. A preliminary high-resolution knowledge of the main locations of the scattering centers can help to specify a radar system. Moreover, it can improve signal processing, even if several scattering centers will be situated within the antenna beamwidth.

## II. FLUCTUATION OF THE TARGET SIGNATURE

Automotive targets like vehicles contain several scattering centers at different locations. The interaction of the backscattered waves depends on the incident angle and the reflectivity of the scattering centers within the same range and angular cell. Strong amplitude and phase fluctuations may occur while the observed target is moving, resulting in a possible loss of detection [1]. Furthermore, the range and angular cell size of the radar system is influencing the target signature. In Fig 1 symbolic scattering centers of a car are depicted as asterisks. The bounding box represents the borders of one range and angular cell. If the radar sensor illuminates several scattering centers within one cell, a small lateral displacement (in y-direction) will result in amplitude fluctuation. By adapting the bandwidth and the angular resolution to the location of the main scattering centers this effect can be reduced, and the target signature can be stabilized.

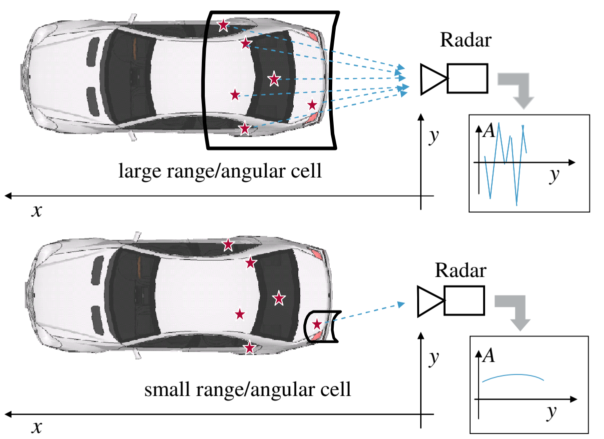


Figure 1. Influence on amplitude fluctuations of the received signal by different range and angular cell size.

## III. MEASUREMENT OF THE SCATTERING CENTERS

To determine the different locations of the scattering centers in a precise way, the principle of synthetic aperture radar (SAR) can be used. SAR enables a range independent cross-range resolution, while a large bandwidth of 7 GHz in these investigations gives a range resolution of approximately 3 cm. In [2] the influence of the carrier frequency (24/77 GHz) and the bandwidth on the scattering centers location at a

Mercedes-Benz S-Class using SAR processing have been compared. To analyze as well the scattering center distribution in elevation, a combination of SAR and digital beam forming (DBF) will be presented in this paper. To compare these results with those of a radar having conventional antennas, a mechanical scanned antenna is applied to scan in azimuth and elevation angles.

### A. *Measurement Setup*

Fig. 2 (a) shows the basic block diagram of the measurement setup, Fig. 2 (b) the mechanical setup used for the SAR measurement. The system consists of an FMCW radar sensor mounted on a height-adjustable linear drive unit with a maximum driveway of 6 m, the control electronics of the sensor [3], a laptop computer, stepper driver, and stepper motor. The laptop computer starts the measurement procedure with the calibration of the stepper motor and the initialization of the radar sensor via RS-232 commands. Following this, the sensor is positioned to the exact measurement positions, and the measured data of the FMCW radar sensor are retrieved via the control unit. The AD converted time domain signals are then fed to the laptop computer via a USB 2.0 interface for either real-time signal processing or storage on the hard disk for later processing. Fig. 2 (c) depicts the scheme of the mechanical scanning system. A two-axis stepper driver enables to scan in azimuth $\psi$ as well as in elevation $\theta$.

Three different sensor/antenna configurations have been employed for the measurements as described in this paper; these are listed in Table I.

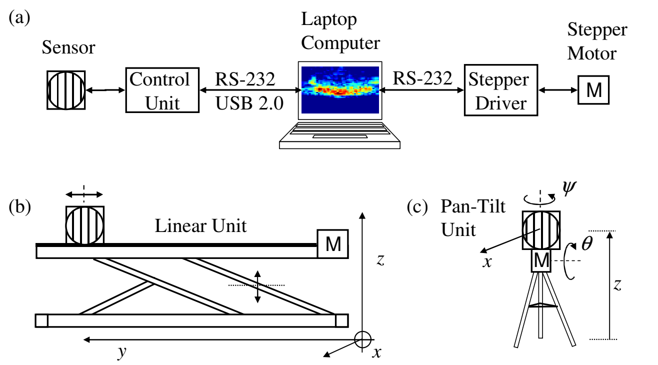


Figure 2. (a) Block diagram of the measurement setup for the scattering center analysis. (b) Scheme of the linear unit for SAR and SAR in combination with DBF processing, (c) scheme of the pan-tilt unit of the mechanical scanning antenna.

For the SAR evaluation (range and azimuth cross range) of the car rear end, a sensor equipped with a folded reflectarray antenna [4] (one-way half power beamwidth (HPBW) of 2.6°, sensor 1 in Table I) was mounted on the linear drive unit. Extending the analysis of the scattering centers to the third dimension (elevation), a sensor with a switched antenna array for digital beamforming in elevation combined with a cylindrical lens was used, see sensor 2 in Table I. The array antenna consists of 32 patch radiators to which the transmit signal is switched successively, together with two continuously receiving antenna elements [5]. With this concept an equivalent aperture of 64 antennas elements is formed, and delay&sum beamforming can be applied to process the position of scattering centers also in elevation.

TABLE I. TECHNICAL DATA OF SENSOR AND MEASUREMENT SETUP

| **Parameter** | **FMCW Radar Sensor Setup** | | |
|---|---|---|---|
| | ***SAR Sensor 1*** | ***3D Sensor 2*** | ***Mech. Scanning Sensor 3*** |
| Start frequency | 73.5 GHz | 74 GHz | 77 GHz |
| Bandwidth | 7 GHz | 4.8 GHz | 2 GHz |
| Theor. min. range cell size | 2.1 cm | 3.1 cm | 7.5 cm |
| Antenna HPBW (azimuth) | 2.6° | 6° | 2.6° |
| Antenna HPBW (elevation) | 2.6° | 2.5° (a) | 2.6° |
| Step size | 18.6 mm | 9 mm | 1° (AZ), 2° (EL) (b) |

(a) DBF: delay&sum (32 TX, 2 RX antenna elements)

(b) Angular stepping size in azimuth (AZ) and elevation (EL)

To get a "conventional" two dimensional image of the targets, radar sensor 3 of Table I was attached to the pan-tilt unit. The antenna was the same folded reflectarray antenna as with sensor 1, only the operation was performed with a smaller bandwidth around 77 GHz

### B. *SAR processing of the car rear end*

In the following, the rear ends of two target vehicles are investigated by the strip map mode of the SAR processing [6] using sensor 1 (see Table I). These targets are a Smart-for-Two (A) and a Mercedes-Benz S-Class (B). The height of the linear unit was adjusted to 0.6 m, and the maximum measurement drive way was 2.3 m. Target A and B were placed in front of the radar sensor at distances of 12.7 m and 10.5 m, respectively. Target A had a small lateral misalignment of -4°.

In Fig. 3 the two-dimensional SAR measurement results of the rear ends of the two cars are depicted; the exact contours of the vehicles under test are overlaid in white color. The scattering analysis shows the main scattering centers in the regions of rear tire tread, rear lights, and the license plate. Furthermore, both targets exhibit scattering centers at the windshield pillars in combination with the rear view mirrors. Due to symmetry, these scattering centers should appear on both sides, the misalignment of target A, however, causes a reduced received power of these scattering centers because they were masked by the vehicle rear end.

### C. *3D-measurement of the vehicle side*

Scattering centers are not only located in one plane, as depicted in Fig. 3, but also at different heights. Hence, the backscattered radar signals are influenced as well by the elevation diagram of the antenna. To determine the scattering center location of the car side, DBF in combination with strip map SAR has been used. As in previous measurements, the scattering centers have been obtained in azimuth by SAR processing and in elevation by DBF processing.

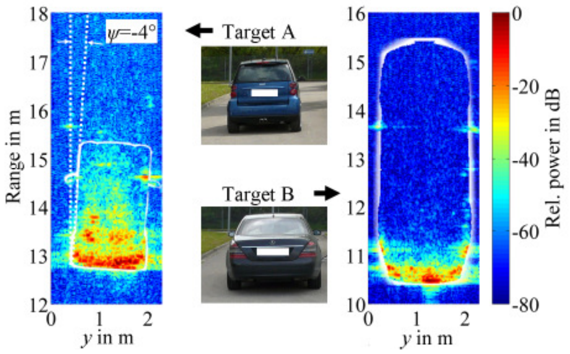


Figure 3. SAR processed radar images of the vehicle rear ends at 77 GHz with a bandwidth of 7 GHz.

The measurement took place on a standard asphalted lane with the sensor at a height of 0.6 m above the ground ($z = 0$ m). The car was located at a distance of 5 m in front of radar sensor 2. The radar sensor, using horizontal polarization, was moved in $y$-direction from $y$=0 m to 5.8 m in 9 mm steps. A corner reflector (designated with "A" in Fig. 4) was arranged in line of sight with the radar sensor at a distance of 12 m and a height of 0.9 m ($z = +0.3$ m); its radar cross section (RCS) was +20 dBsm at 77 GHz. Furthermore, a corner reflector designated as "B" (RCS of +30 dBsm at 77 GHz) was located at the road surface at a distance of 10 m hidden behind the vehicle. These two corner reflectors were used as reference targets.

In Fig. 4 the measurement results are illustrated. To clearly see the major contributing scattering centers, the minimum displayed relative power is -10 dB. The results contain reflection regions at different heights. Corner reflector A and B of Fig. 4 seem to consist of several scattering centers in height, however, this discretisation effect is caused by the SAR processing, because the measurement data were processed separately for each elevation angle. In the measurement results, corner reflector B appears quite clearly but with reduced amplitude compared to reflector A due to multipath propagation.

Reflection regions C to I marked in Fig. 4 stem from signal reflections of the vehicle. The door outer skin C has a strong reflection region starting close to the front wheel and ending close to the back wheel. However, there are two remarkable disruptions of the continuous backscattering at the door gap D of the front door. Furthermore, region C is a dynamic scattering region, depending on the incident angle of the impinging wave front. This means, in case of a laterally moving car a sliding scattering center occurs within the shortest distance between vehicle and the radar sensor. At some incident angles, the waves are reflected away from the sensor, and no radar response will be detected.

Furthermore, there are distributed reflection regions at the side sill beneath the outer skin of the door, represented by E. Moreover, pseudo reflection regions F are located below the road surface caused by reflections at the door via the road surface.

The front wheel H as well as the rear wheel G exhibit distinct backscattering characteristics. Mainly the wheel rims with the tire tread G, as well as the wheel suspension H show strong reflections. With this vehicle orientation, the wheel-arch panel had no significant influence on the backscattering of the vehicle. The reflection region I arises at both the front wheel and the rear wheel also resulting from reflections at the road surface.

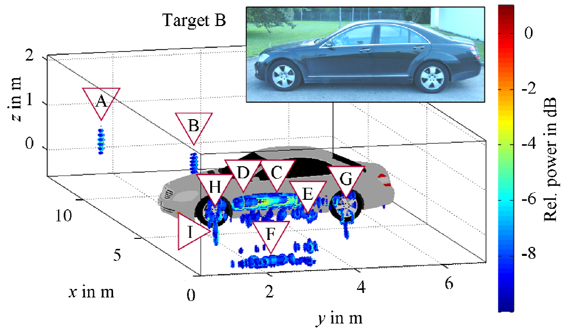


Figure 4. DBF+SAR processed radar image of the vehicle side view (target B) at 77 GHz with a bandwidth of 4.8 GHz.

### D. *Measurement by a mechanical scanning radar*

The measurements as described above provide a fine cross range resolution (azimuth) which in principle is independent of the distance of the target. Real automotive radar systems, however, cannot use the SAR principle; consequently, the lateral resolution is proportional to the distance, while the range resolution is the same for all distances. This section therefore compares the SAR measurements of targets A and B with the response of a conventional radar sensor. Imaging methods of actual sensors like multibeam operation or digital beamforming are replaced by mechanical scanning (sensor 3 in Table I).

For advanced security systems, emergency breaking is the preferred option if the distance is large enough; at smaller distances, evading maneuvers may be a better choice. To this end, however, it is necessary to know as exactly as possible the dimensions and orientations of cars in front of the sensor. This can be easily determined based on the SAR results, and the measurements described below should also check to what extent this is possible with a conventional sensor arrangement.

For the measurements, the sensor was positioned at a height of 0.6 m above ground. The azimuth and elevation step size of the pan-tilt were adjusted to 1° and 2°, respectively. The single path beamwidth of the antenna of 2.6° results in a two-way diagram with a 3 dB widths of 1.85°.

#### 1) *Influence of the elevation angle on the target signature*

The elevation angle influence on the target signature of target B has been investigated from -2° to +2°. In practice, negative elevation angles occur during deceleration (the car tilts down somewhat) and positive angles during acceleration.

The left vehicle side was oriented towards the sensor at a distance of 10 m with its rear end in line with the radar. Fig. 5 shows the measurement results of target B with the overlaid contour in white color. At an elevation angle of 0°, the front and rear wheel, the door pillar, and the rear end exhibit strong reflecting regions. Increasing the elevation angle to +2° reduces the scattering center size of the rear end, caused by a lowered reflection of the rear light unit. Furthermore, the *right* front and rear wheels disappear completely due to the changed incident angle and the shadowing effect of the body shell. At the same time, the windshield (A-pillar), center (B-pillar) and rear pillar (C-pillar) have increased reflectivity. Adjusting an elevation angle of -2°, the reflections at these pillars nearly disappear completely. However, the front and rear wheel on the *right* side of the vehicle emerge due to multipath propagation between car body and ground. Due to a reduction of the reflections at the rear end of the vehicle, the rear wheel appears in a more distinct way. Although some scattering centers change their reflectivity as a function of elevation angle, the wheels still show remarkable reflections to estimate the target position.

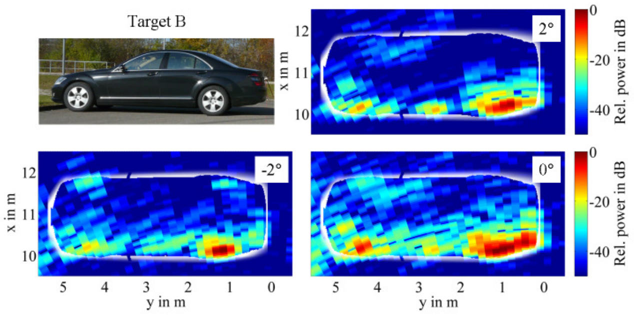


Figure 5. Elevation influence on the scattering centers of the vehicle side view using a mechanical scanning radar at 77 GHz using a bandwidth of 2 GHz.

### 2) *Determination of the target orientation*

Fig. 6 depicts measurement results of targets A and B at a distance of 10 m and a yaw angle of 30°. The contour of each vehicle is overlaid in white color. For both targets, it can be seen that the scattering centers are arranged in an L-shape structure from which, in principle, the orientation and the dimension of the vehicle can be derived. In Figure 6 right, however, not the entire length of the vehicle can be recognized clearly because of the shallow incident angle of the radar signal at the outer panel of the fender. This mirror effect causes that only the left front wheel shows strong reflections. In summary, both targets exhibit strong reflections at the left front and rear wheel, the rear light units, and in the region of the license plate. It can be seen that using a bandwidth of 2 GHz in combination with an angular resolution of approximately 2° (two-way radiation diagram) enables to determine the target contour and orientation at this distance.

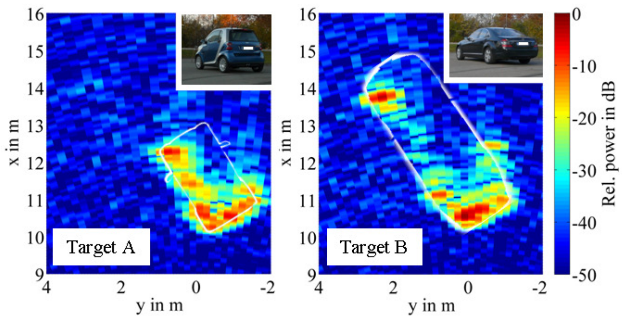


Figure 6. Influence of the target type using a mechanical scanning radar at 77 GHz with a bandwidth of 2 GHz.

## CONCLUSION

3D scattering centers of two different vehicles have been evaluated using SAR, and the combination of SAR and DBF. The results show that main scattering centers are located at the wheels, the regions around the license plate, the door outer panel, the windshield pillar, center pillar, rear pillar, and the light units. Furthermore, it has been shown that multipath propagation enables an indirect detection of scattering centers. The comparison between the measurement results of the SAR processing and the mechanical scanning radar confirmed similar main scattering centers. Furthermore, the measurement results show that the contour of a vehicle and the orientation can be determined at a distance of 10 m with a bandwidth of 2 GHz and an angular resolution of approximately 2°.

## ACKNOWLEDGMENT

This work has been funded by the German Federal Ministry of Education and Research (BMBF) under the joint project Radar on Chip for Cars (RoCC). The authors wish to thank Daimler AG, Ulm for the sub-contract and for providing target cars.

## REFERENCES

[1] Skolnik, M.: “Radar Handbook,” McGraw-Hill, 2nd edition, 2003

[2] M. Andres, P. Feil, W. Menzel, H.-L. Bloecher, J. Dickmann, “Analysis of Automobile Scattering Center Locations by SAR Measurements,” *Radar Conference*, Kansas City, USA, May 2011

[3] W. Mayer, A. Gronau, W. Menzel, H. Leier, ”A Compact 24GHz Sensor for Beam-Forming and Imaging,” *9th International Conference on Control, Automation, Robotics and Vision ICARV 2006*; Singapore, Dec. 2006

[4] S. Dieter, C. Fischer; W.Menzel, “Design of a folded reflectarray antenna using Particle Swarm Optimization,” *40th European Microwave Conference*, Paris, September 2010

[5] P. Feil, T. Chaloun, “Active Switched Antenna Array for 77 GHz Digital Beamforming Radar,” *5th European Conference on Antennas and Propagation*, Rome, Italy, April 2011

[6] P. Feil, T. Kraus, W. Menzel, “Short Range mm-Wave SAR for Surveillance and Security Applications,” in *Proc. 8th European Conference on Synthetic Aperture Radar*, Aachen, Germany, June 2010